PROCEEDINGS, 49th Workshop on Geothermal Reservoir Engineering
Stanford University, Stanford, California, February 12-14, 2024
SGP-TR-227

Entropy production as a comprehensive indicator to address epistemic uncertainties – A case study of The Hague, Netherlands

Ryan Santoso[1,2,*], Denise Degen[1], Dominique Knapp[3], Renate Pechnig[3], Florian Wellmann[1,4]

[1]Computational Geoscience, Geothermics, and Reservoir Geophysics (CG3), RWTH Aachen University, Germany
[2]Geothermal Energy and Geofluids (GEG), ETH Zurich, Switzerland
[3]Geophysica Beratungsgesellschaft mbH, Germany
[4]Fraunhofer IEG, Germany

*Corresponding author: ryan.santoso@cgre.rwth-aachen.de

Keywords: Entropy Production, Uncertainty Quantification, Global Sensitivity Analysis, Epistemic Uncertainty, Thermo-Hydraulic

ABSTRACT

We present a global sensitivity analysis with an entropy production objective function to improve our understanding of transient thermo-hydraulic processes in geothermal reservoirs under epistemic uncertainties. The entropy production describes the contributions of the irreversible heat transfer and the fluid flow friction. As a global sensitivity analysis demands numerous model runs to measure the significance of each physical parameter, we employ the non-intrusive reduced basis method to construct a surrogate model to decrease the computational cost. We test the application for a geothermal reservoir study in The Hague, Netherlands. The use of a surrogate model provides more than eight orders of magnitude speed-up, enabling an efficient global sensitivity analysis. With the use of the entropy production as the objective function, we can capture important parameters contributing to both the thermal and the hydraulic process for all time steps. The use of either only the pressure or the temperature state as an objective function in the global sensitivity analysis fails to identify important parameters contributing to the thermo-hydraulic process.

1. INTRODUCTION

Global sensitivity analyses have been used before to improve the understanding of physical processes, captured via numerical simulations, by characterizing the contribution of input parameters on the variations of an objective function (Saltelli et al., 2019). However, they provide us with the challenge is of selecting a comprehensive objective function that leverages the understanding of the desired physical processes (Degen et al., 2021b; Wainwright, 2014). For improving the knowledge of transient thermo-hydraulic processes in geothermal reservoirs, the entropy production provides useful insight (Börsing et al., 2017; Bejan, 2013; Regenauer-Lieb et al., 2010). The entropy production, derived from the Second Law of Thermodynamics, characterizes the thermodynamic state and the irreversibility of a system (Börsing et al., 2017; Bejan, 2013; Regenauer-Lieb et al., 2010). It offers an abstraction to describe multi-physics processes, including thermo-hydraulic processes, in geothermal applications. Huang and Wellmann (2021), Niederau et al. (2019), Börsing et al. (2017), and Wellmann and Regenauer-Lieb (2012) successfully utilize the entropy production to identify instabilities in hydrothermal systems, to discern a shift from conductive to convective processes, and to indicate variations in geometries and the heterogeneity of the permeability. In this paper, we use the entropy production to gain an understanding of the transient thermo-hydraulic process in The Hague, Netherlands, in the context of the heat extraction process.

The spatio-temporal understanding of the thermo-hydraulic process in geothermal applications is often gained through numerical simulations as measurement data is limited and sparse (Beer et al., 2023; Degen et al., 2023; Willcox et al., 2021; Degen et al., 2021b; Schulte et al., 2020). The numerical simulation inherently carries uncertainties, particularly *epistemic uncertainties* (uncertainties caused by inaccurate characterization of physical parameters and incomplete knowledge of physical processes) (Degen et al., 2022., 2021c; Willcox et al., 2021; Schulte et al., 2020). Inspired by the work of Niederau et al. (2019) and Börsing et al. (2017), we can further use the entropy production to analyze which material properties dominate the transient thermo-hydraulic process. This, in turn, will help for future analysis investigating the epistemic uncertainties.

The global sensitivity analysis (GSA) becomes an essential tool for this purpose (Degen et al., 2021b; Wainwright, 2014). It characterizes the impact of parameters and their correlation with respect to an objective function that is used for improving the system understanding (Degen et al., 2022, 2021c; Saltelli et al., 2019; Wainwright, 2014). We use the variance-based Sobol sensitivity analysis (Sobol, 2001) since the transient thermo-hydraulic problem is non-linear, which eliminates the use of local sensitivity analyses (Degen et al. 2022; 2021c; Saltelli et al., 2019).

Given the computational cost of performing global sensitivity analyses (Degen et al., 2021a; 2021b; 2021c), we use a surrogate model constructed through the non-intrusive reduced-basis (NI-RB) method. The NI-RB method is a model order reduction (MOR) technique that reduces the spatial and temporal degrees of freedom of parameterized partial differential equations (PDEs) such as thermo-hydraulic problems. It represents the solution of these PDEs as a linear combination of basis functions and weights (Swischuk et al., 2019; Wang et al., 2019; Hesthaven and Ubbiali, 2018). The basis functions contain the structure of the physical processes, and the weights are calculated using a non-intrusive approach, such as a machine learning model (Swischuk et al., 2019; Wang et al., 2019; Hesthaven and Ubbiali,

2018). This method ensures physical consistency in the surrogate model's predictions (Degen et al., 2023; Willcox et al., 2021; Swischuk et al., 2019; Wang et al., 2019; Hesthaven and Ubbiali, 2018).

We aim to understand the transient thermo-hydraulic process in The Hague, Netherlands under the influence of epistemic uncertainties using global sensitivity analysis. The Hague, Netherlands is in the West Netherland basin where the main interest for the heat extraction process is on the Delft Sandstone (Lower Cretaceous layer) (Willems et al., 2020; Mottaghy et al., 2011). The recoverable heat from the Delft sandstone is expected to provide heating for 6000 houses in the DenHaag Zuidwest district and the planned heat extraction process involves an injection-production procedure using a doublet setup (Mottaghy et al., 2011).

The structure of this paper is as follows: In Section 2, we show the thermo-hydraulic formulation and present the concepts of entropy production and global sensitivity analyses. The sensitivity analysis results are shown in Section 3. It is followed by discussions in Section 4 and conclusions in Section 5.

2. MATERIALS AND METHODS

In this section, we first present the thermo-hydraulic formulation, describing the heat extraction process. It is then followed by introducing the concept of entropy production for hydrothermal flow characterization. We also provide a brief introduction to the concept of variance-based global sensitivity analysis. For the surrogate modelling construction, we illustrate the concept of the non-intrusive reduced-basis method.

2.1 Transient thermo-hydraulic process

We solve a 3-D coupled fluid flow in a porous medium and the heat transfer equation for modeling the transient thermo-hydraulic processes in geothermal reservoirs as it is presented in Cacace and Jacquey (2017). The fluid density and fluid viscosity are dependent on the pressure and temperature, following the IAPWS correlation (Cacace and Jacquey, 2017). The solid thermal conductivity is dependent on the temperature, and is mathematically expressed as follows (Clauser, 2003):

$$\lambda_s = \begin{cases} \left(\frac{770}{350+T\,[^oC]} + 0.7\right)\left[\frac{W}{m\,^oC}\right] & T > 800\ ^oC \\ \left(\left[\frac{770}{350+T\,[^oC]} + 0.7\right] \times \left[\frac{\lambda_s^{ref}}{2.78}\left(1 - \left(\frac{T\,[^oC]-20}{800-20}\right)\right) + \left(\frac{T\,[^oC]-20}{800-20}\right)\right]\right)\left[\frac{W}{m\,^oC}\right] & T < 800\ ^oC \end{cases}, \quad (1)$$

where λ_s^{ref} is the reference solid thermal conductivity at 20 °C and T is the temperature. We use the finite element method with a hexahedral grid (HEX8) to solve for the pressure and temperature states. To perform these computations, we utilize the open-source software GOLEM, a MOOSE-based application (Lindsay et al., 2022), developed by Cacace and Jacquey (2017).

2.2 Entropy production

According to the Second Law of Thermodynamics, the entropy is a measure of the molecular disorder or randomness of a system (Kern and Weisbrod, 1967). Bejan (2013) further formulates the volumetric rate of the total entropy production ($\dot{S}$), a measure of increase in entropy associated with irreversible processes, in a saturated porous medium. It is expressed as a linear combination of the irreversible heat transfer $\dot{S}_{therm}$ and the fluid flow friction $\dot{S}_{visc}$ contribution:

$$\dot{S} = \dot{S}_{therm} + \dot{S}_{visc} = \frac{\left[\lambda_f{}^{\emptyset} + \lambda_s{}^{1-\emptyset}\right]}{\left(\frac{T_{top}+T_{bottom}}{2}\right)^2}(\boldsymbol{\nabla} T)^2 + \frac{\eta}{\boldsymbol{k}\left(\frac{T_{top}+T_{bottom}}{2}\right)}\boldsymbol{v}^2, \quad (2)$$

where λ_f is the fluid thermal conductivity, η is the fluid dynamic viscosity, $\boldsymbol{k}$ is permeability, $\boldsymbol{v}$ is the velocity, T_{top} is the temperature at the top boundary, T_{bottom} is the temperature at the bottom boundary.

With the use of the entropy production concept, Börsing et al. (2017) show the temporal evolution of a system from a conductive to a convective state. Furthermore, Niederau et al. (2019) and Wellmann and Regenauer-Lieb (2012) demonstrate the use of the entropy production to analyze the impact of permeability and geometric uncertainties on transient thermo-hydraulic processes. Considering the success of these works, we further use the entropy production as an objective function in global sensitivity analyses, to improve our understanding of the transient thermo-hydraulic process in The Hague, Netherlands. This understanding is important to ensure safe and efficient injection-production operations in this region.

2.3 Global Sensitivity Analysis

The idea behind global sensitivity analyses is to identify parameters that have a significant impact on the model response and determine potential parameter correlations based on their contributions to the variation of an objective function. Through this identification, we can gain insights into the physical processes occurring in our system (Degen et al., 2021b; Wainwright, 2014).

The identification of significant parameters is based on sensitivity indices, defined in Sobol (2001). The total sensitivity index S_T measures the contribution of each parameter on an objective function, including its interaction with other parameters. It is mathematically expressed as

$$S_{Ti} = 1 - \frac{\mathrm{Var}_{\boldsymbol{\mu}_{\sim i}}\left[\mathbb{E}_{\boldsymbol{\mu}_i}[f(\boldsymbol{\mu};t)|\boldsymbol{\mu}_{\sim i}]\right]}{\mathrm{Var}\,[f(\boldsymbol{\mu};t)]}, \tag{3}$$

where $f(\boldsymbol{\mu};t)$ is an objective function focusing on, for instance, physical processes, $\mathrm{Var}[\cdot]$ is the variance, $\mathbb{E}[\cdot]$ is the expectation, and $\boldsymbol{\mu}_{\sim i}$ represents all parameters except the i-th parameter. The first-order sensitivity index S measures the contribution of each parameter without considering its correlation with other parameters, mathematically written as:

$$S_i = \frac{\mathrm{Var}_{\boldsymbol{\mu}_i}\left[\mathbb{E}_{\boldsymbol{\mu}_{\sim i}}[f(\boldsymbol{\mu};t)|\boldsymbol{\mu}_i]\right]}{\mathrm{Var}\,[f(\boldsymbol{\mu};t)]}, \tag{4}$$

The detailed algorithm and sampling method to compute the sensitivity indices is presented in Saltelli (2002). We utilize the SALib Python library for conducting variance-based global sensitivity analysis, employing the Saltelli sampling method (Herman and Usher, 2017). To reduce statistical error, we use 100,000 realizations per parameter, resulting in 2,800,000 total realizations for the entire global sensitivity analysis.

2.4 Case study: reservoir simulation for The Hague, Netherlands

We are interested in improving our understanding of the transient thermo-hydraulic process in The Hague, Netherlands, specifically in the Delft sandstone layer, during the injection-production process using doublet setup. For this purpose, Mottaghy et al. (2011) develop two geological models: a regional geological model and a reservoir model. The regional geological model is used for investigating the temperature distribution across the region before the extraction process and the reservoir model, embedded within the regional geological model, is employed to evaluate the heat produced during the injection-production process.

Based on Mottaghy et al. (2011), the regional geological model of The Hague, Netherlands spans 22.5 km east-west and 24.3 km north-south as depicted in Figure 1. It consists of nine layers with a total model depth of 5 km and has 2,485,913 nodes (hexahedral grid), see Figure 1. The solid density for all layers is 2,570 kg/m^3, the solid heat capacity 960 J/(kg K), the porosity is 0.001, and the permeability is 1×10^{-17} m^2. The uncertain parameters in the regional model are the solid thermal conductivity of each layer (shown in Table 1) and the heatflow at the bottom of the model, which varies between 0.06 and 0.07 W/m² (Mottaghy et al., 2011).

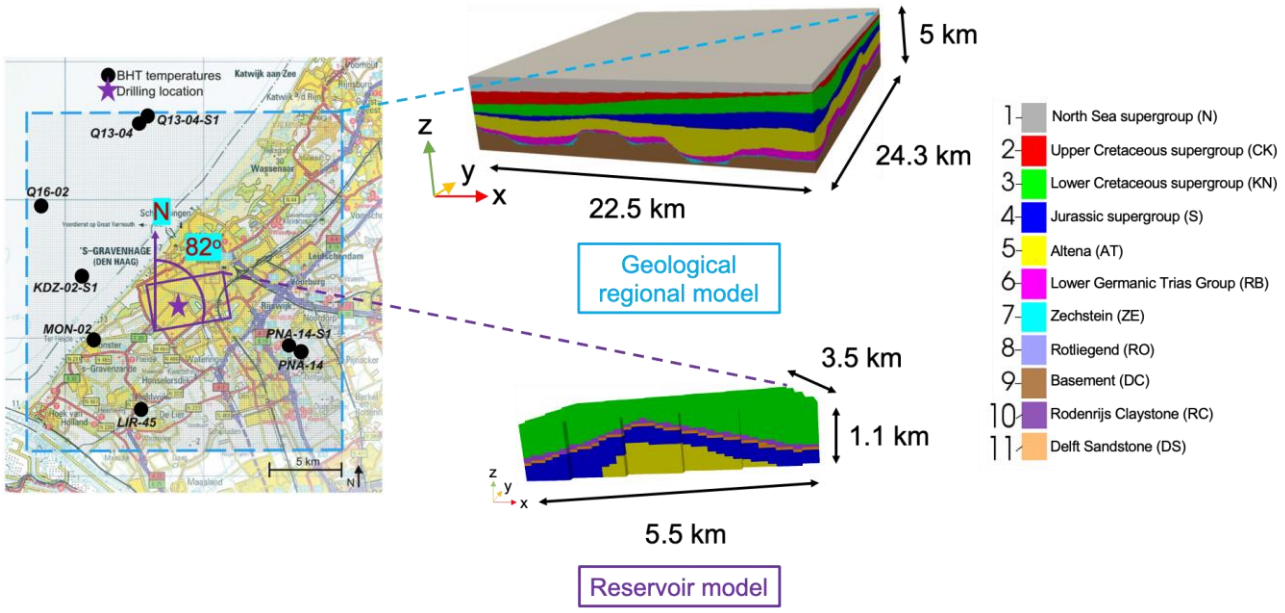

Figure 1: The geological model of The Hague, Netherlands, adopted from Mottaghy et al. (2011). The top model (denoted with a light blue font color) is the regional geological model and the lower model (denoted with a purple font color) is the reservoir model.

The reservoir model has an extend of 5.5 km × 3.5 km × 1.1 km, and 21,275 nodes (hexahedral grid), see Figure 1. It consists of five layers (Figure 1). The solid density and solid heat capacity for all layers in the reservoir model are the same as in the regional model. The uncertain parameters in the reservoir model are the permeability of the Delft Sandstone and the solid thermal conductivities of the adjacent layers (Table 1). The thermal conductivity of the Rodenrijs Claystone and the Delft Sandstone is set to their mean values.

Table 1: The rock properties for each layer in the regional geological model and the reservoir model in The Hague, Netherlands, obtained from Mottaghy et al. (2011).

Regional geological model		Reservoir model			
Geological layers (from top to bottom)	**Solid thermal conductivity [W/(m K)]**	**Geological layers (from top to bottom)**	**Solid thermal conductivity [W/(m K)]**	**Porosity**	**Permeability [m^2]**
North Sea Supergroup (N)	1.8 – 4.0	Lower Cretaceous Supergroup (KN)	1.8 – 3.7	1×10^{-3}	1×10^{-17}
Upper Cretaceous Supergroup (CK)	1.7 – 3.0	Rodenrijs Claystone (RC)	3.5	1×10^{-3}	1×10^{-17}
Lower Cretaceous Supergroup (KN)	1.8 – 3.7	Delft Sandstone (DS)	5.6	0.15	3×10^{-14} - 2×10^{-12}
Jurassic Supergroup (S)	2.3 – 4.9	Jurassic Supergroup (S)	2.3 – 4.9	1×10^{-3}	1×10^{-17}
Altena (AT)	1.6 – 2.7	Altena (AT)	1.6 – 2.7	1×10^{-3}	1×10^{-17}
Lower Germanic Trias Group (RB)	1.5 – 4.7				
Zechstein (ZE)	1.7 – 5.0				
Rotliegend (RO)	2.0 – 4.8				
Basement (DC)	1.5 – 3.9				

Both the regional and the reservoir model are saturated with water, which has a density of 1,000 kg/m^3, a thermal conductivity of 0.65 W/(m K), and a heat capacity of 4193.5 J/(kg K). The injection-production activity is conducted only in the Delft Sandstone layer with an injection rate of 41.67 – 45.83 L/s and an injection temperature 35 – 40 °C. The range for the injection rate and the injection temperature are obtained by combining values from Veldkamp et al. (2016) and Mottaghy et al. (2011).

While utilizing the same models as Mottaghy et al. (2011), our study incorporates different scenarios, with a particular focus on modifying the top and bottom boundary conditions of the reservoir model. Unlike the fixed top boundary condition of the reservoir model of 55.8 °C in Mottaghy et al. (2011), we recognize that the top reservoir layer is part of the Lower Cretaceous Supergroup (KN), and this layer features an uncertain thermal conductivity. Similarly, we refrain from assigning a fixed value for the bottom boundary condition of the reservoir model. Variability in the top and bottom boundary condition values yields variability in pressure and temperature state. The procedures to include these uncertain boundary conditions into the transient thermo-hydraulic simulations for The Hague is the following (for each realization):

1. Conduct a steady-state thermal simulation of the regional geological model to obtain the entire temperature state.
2. Transfer the temperature values at the depth slice corresponding to the top of the reservoir model to establish the top boundary condition for the reservoir model. Consequently, the temperature at the top boundary varies spatially.
3. Calculate the heat flow at the depth slice corresponding to the bottom of the reservoir model and transfer these values to determine the bottom boundary condition of the reservoir model. Hence, the calculation of heat flow at the bottom boundary considers a spatial variation of the temperature.
4. Execute a transient thermo-hydraulic simulation of the reservoir model using the boundary values obtained from the regional geological model.

With this setup, we provide a more accurate characterization of the produced heat, accounting for uncertainties of the reservoir model's boundary conditions. Moreover, we do not merge the two models since we do not have enough measurement data to extrapolate the reservoir model layers into the regional model layers.

2.4.1 Objective functions

In this paper, we aim to investigate the influence of various objective functions for the global sensitivity analysis to improve our understanding of thermo-hydraulic processes. In Figure 2, we illustrate all performed global sensitivity analyses.

We split the period of analysis into two phases:

- Before injection: in this period, since the The Hague region is conductive, there is no flow occurring (Mottaghy et al., 2011). The main heat transfer mechanism here is the heat conduction.
- During injection: in this period, there is a flow due to the injection and production process in the doublet setting.

For each period, we perform the global sensitivity analysis with four different objective functions:

- Total thermal energy: The total thermal energy is calculated as the sum of the temperature of the entire model. This objective function produces a sensitivity analysis illustrating changes in the overall temperature distribution of the reservoir model, treating each region equally.
- Total kinetic energy: This objective function is computed as the sum of the pressure of the entire model. It generates a sensitivity analysis that outlines changes in the overall pressure distribution of the reservoir model, with equal consideration given to every region.
- Total thermal and kinetic energy: We propose this objective function to capture simultaneous changes in both the pressure and the temperature, this objective function assigns equal weights to the temperature and pressure responses across the entire reservoir model. It is calculated as the sum of the temperature and pressure of the entire model.
- Total entropy production: Inspired by the derivation in Section 2.2, this objective function has a similar purpose as the "total thermal and kinetic energy " objective function. However, for the total entropy production, the gradient of the temperature and pressure is used instead of the temperature and pressure themselves.

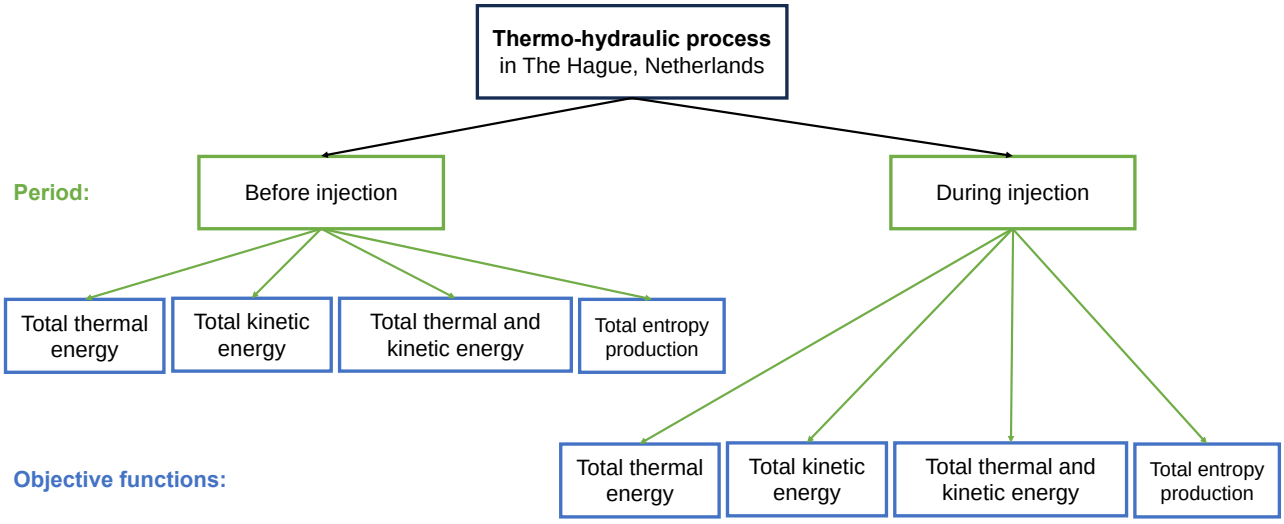

Figure 2: Analysis phases and objective functions used in the global sensitivity analysis for understanding the thermo-hydraulic process in The Hague, Netherlands.

2.5 The non-intrusive reduced-basis method

The non-intrusive reduced-basis (NI-RB) method constructs a surrogate model that provides a map from the parameters $\boldsymbol{\mu}$ and the time t to the solution of, for instance, a thermo-hydraulic problem, which is represented by the pressure P and the temperature T. Using the temperature and pressure state, we create an additional mapping to a quantity of interest, the entropy production $\dot{S}$. There are 13 parameters, including uncertain rock properties and operation-related parameters (injection rate and injection temperature), which serve as the inputs of the surrogate model.

The NI-RB method expresses a solution as a linear combination of basis functions and coefficients, which is mathematically written as follows:

$$\boldsymbol{z}(\boldsymbol{x}, t; \boldsymbol{\mu}) = \sum_{k=1}^{r} V_k(\boldsymbol{x})\ \alpha_k(t, \boldsymbol{\mu}), \tag{3}$$

where $\boldsymbol{z}(\boldsymbol{x}, t; \boldsymbol{\mu}) \in \mathbb{R}^{N_t \times N_x}$ is the solution. Here N_t are the number of time steps and N_x are the number of nodes, $\boldsymbol{x}$ are the spatial coordinates, $\boldsymbol{V}(\boldsymbol{x}) \in \mathbb{R}^{N_x \times r}$ are the basis functions with r being the reduced dimension, and $\boldsymbol{\alpha}(t, \boldsymbol{\mu}) \in \mathbb{R}^{r \times 1}$ being the coefficients. The basis functions are obtained by applying a Proper Orthogonal Decomposition (POD) on the snapshots of either the solution of the thermo-hydraulic problem or a quantity of interest. For calculating the coefficients, we use a Neural Network. The detailed construction steps are described in Wang et al. (2019). Figure 3 shows an example of the NI-RB surrogate model for the temperature state. We use the Tensorflow Python library (Abadi et al., 2015) to construct the Neural Network and Bayesian Optimization with Hyperband (BOHB), developed by Falkner et al. (2018), implemented in the bohb-hpo Python library (Karakaşlı, 2020). The BOHB method is used to optimize the hyperparameters of the Neural Network (e.g. learning rate, number of epochs, number of neurons, number of layers, and batch size). To construct the NI-RB surrogate model for The Hague, we utilize 300 training samples and 75 test samples, each comprising 302 time steps. The generation of these training and test samples was carried out on 48 cores of the CLAIX High-Performance Computing (HPC)

infrastructure, leveraging Intel Xeon Platinum 8160 Processors ("SkyLake"). The computational process consumed 96 GB RAM and an average compute time of 5 hours for each realization.

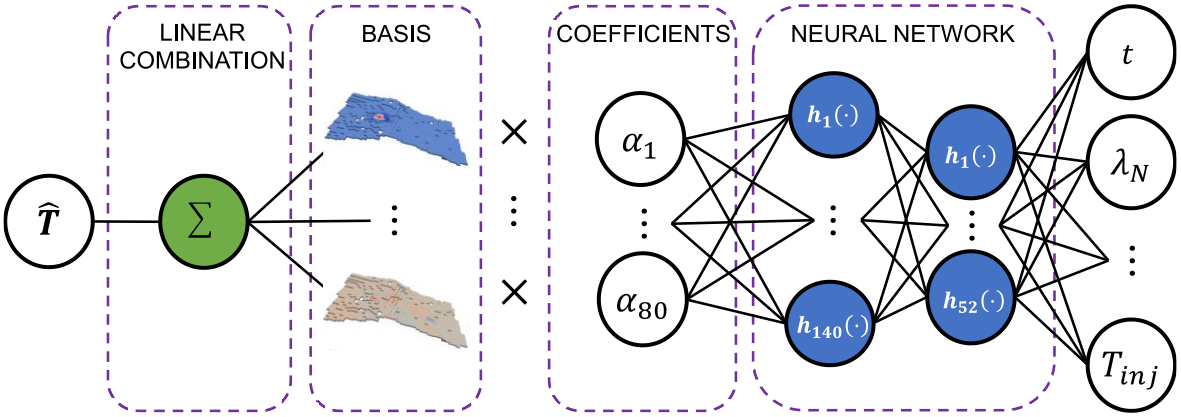

Figure 3: The NI-RB surrogate model for the temperature distribution of The Hague case study. We only show the Delft Sandstone layer in the basis functions to highlight the injection-production process.

3. RESULTS

In this section, we present the results of our global sensitivity analyses, leveraging the NI-RB surrogate models to significantly reduce computational costs. Initially, we present the performance metrics of the surrogate models employed for the global sensitivity analysis. This is followed by the global sensitivity analysis results themselves.

3.1 Performances of surrogate models

Before performing any global sensitivity analysis, it is imperative to ensure the efficiency of evaluating our objective function. In this context, we approximate the pressure, temperature, and entropy production, consecutively, using the NI-RB method. The entropy production is a quantity derived from the pressure and temperature state. The entropy production surrogate model is constructed to facilitate a later comparison of the efficiency between calculating the entropy production function using both the pressure and temperature surrogate models and using the dedicated entropy production surrogate model. The performance metrics for each surrogate model are presented in Table 3 and the corresponding architectures are shown in Table 4. The offline time is defined as the time needed to construct a surrogate model including the time for the generation of training and test samples. The online time is defined as the time spent to predict a new case. The training of the surrogate model and online phase are conducted using a single core on an Apple Macbook Pro with a M1-chip and 8 GB RAM.

The computation of the entropy production from a given pressure and temperature solution (coming from the pressure and temperature surrogate models), utilizing a finite-difference scheme for the gradient calculation, requires 2.03 seconds of computation time. The overall offline time is 4.6×10^3 seconds $+ 8.4 \times 10^3$ seconds $+ 6.8 \times 10^6$ seconds $= 6.81 \times 10^6$ seconds, accounting for the construction of both the pressure and temperature surrogates and the generation of the training and test samples. In contrast, using an entropy production surrogate model, we can predict a new entropy production solution at a single time step within 1.3×10^{-3} seconds with 3.4×10^4 seconds $+ 6.8 \times 10^6$ seconds $= 6.83 \times 10^6$ seconds of offline time. Therefore, it is more efficient to use an entropy production surrogate model to perform the global sensitivity analysis, especially considering that the offline phases of both approaches require a similar amount of resources.

Table 3: Performance of the surrogate models used in the global sensitivity analysis. The values denoted with a red font color represent the total time needed to generate the training and test samples, while the black color represents the time needed to construct a surrogate model. The values in the brackets denote the time needed for a trained surrogate model to predict a new case with 302 time steps and the ones outside the brackets denote the time needed to predict a new case for a single time step.

Surrogate model	Number of basis functions	Approximation error L_2	Offline time [s]	Online time [s]
Pressure	31	3.4×10^{-2}	$4.6 \times 10^3 + 6.8 \times 10^6$	6.3×10^{-4} (1.9×10^{-1})
Temperature	80	3.4×10^{-2}	$8.4 \times 10^3 + 6.8 \times 10^6$	5.9×10^{-4} (1.7×10^{-1})

Entropy production	380	2.9×10^{-3}	$3.4 \times 10^{4} + 6.8 \times 10^{6}$	1.3×10^{-3} (4.0×10^{-1})

Table 4: Architectures and hyperparameters of surrogate models used in global sensitivity analysis.

Surrogate model	Neurons in layer 1	Neurons in layer 2	Learning rate	Number of epochs	Batch size
Pressure	92	119	2.9×10^{-5}	46,459	5,337
Temperature	52	140	1.5×10^{-4}	46,768	2,330
Entropy production	48	124	3.8×10^{-5}	41,506	31,613

3.2 Influence of different objective functions at before injection period

In Figure 4a, we show the total sensitivity indices obtained with different objective functions. We only show the total sensitivity indices since there is no significant difference between the first-order values and their associated total sensitivity values, indicating minimal correlations. It is essential to note that, during this period, there is no fluid flow and the heat conduction is the governing process regulating the temperature in the entire reservoir. Since there is no flow before the injection period, we cannot obtain the sensitivity result with the total kinetic energy objective function. The total sensitivity indices depicted in Figure 4a yield the same results for both the total thermal energy, and thermal and kinetic energy objective functions. Using the total thermal and kinetic energy objective function, equal weights assigned to temperature and pressure responses, the sensitivity result is dominated by the temperature response. Parameters, including $\lambda_N, \lambda_{CK}, \lambda_{KN}, \lambda_S, Q$, emerge as significant. Specifically, λ_N, λ_{CK} characterize the heat loss from the reservoir, Q describes the heat entering the reservoir, and λ_S controls the heat influx to the reservoir. Despite the inclusion of the Altena layer (depicted in red in Figure 1) in the reservoir model, its significance is masked by the Jurassic layer (depicted in blue in Figure 1). This is attributed to the fact that the Altena layer is surrounded by the Jurassic layer, making the Jurassic layer the primary contributor controlling the heat influx to the reservoir. Consequently, only the Jurassic layer emerges as a significant parameter.

Upon employing the total entropy production as the objective function, a similar ranking is obtained compared to the total thermal energy, and thermal and kinetic energy objective functions, with the addition of the significant parameter k. Notably, even in the absence of fluid flow before the injection period, a pressure gradient of static water exists within the reservoir. In the entropy production formulation (Equation 2), permeability explicitly appears, and given the pressure gradient of static water, permeability becomes a significant factor, impacting the entropy production. With the importance of permeability, we can now see the contribution of fluid flow towards the transient thermo-hydraulic process in The Hague, Netherlands.

We now compare the use of total entropy production and thermal energy objective functions on the total sensitivity values. The total sensitivity value of the heat flow Q with the total entropy production as the objective function decreases while λ_S increases, compared with the use of the total thermal energy as the objective function. It is attributed to the calculation of T_{bottom} in Equation 2, which utilizes the temperature at the bottom boundary, consisting of the Jurassic and Altena layers, rather than the basement (note that the reservoir spans from the Lower Cretaceous layer to at the Altena layer). Despite this change, both the Jurassic layer and the heat flow Q remain significant since the temperature at at the Jurassic and Altena layers is strongly influenced by the heat flow Q.

The total sensitivity value of λ_N, λ_{CK} increases with the use of total entropy production objective function compared to the use of total thermal energy objective function. It is because the calculation for T_{top} in Equation 2 utilizes temperature at the top boundary, at the intersection between the Upper Cretaceous and Lower Cretaceous layers. This intersection is directly connected to the North Sea layer that controls the heat loss. Consequently, the North Sea layer also emerges as a significant parameter.

As the permeability of Delft sandstone, located in the Lower Cretaceous layer, is the highest and has a range value, the entropy production in the Lower Cretaceous layer is characterized by two components: irreversible thermal and fluid flow friction. The contribution of thermal decreases as the contribution of fluid flow appears, hence, λ_{KN} is significant with smaller value than one from total thermal energy objective function and k is significant.

3.3 Influence of different objective functions during injection period

We observe no change in the sensitivity results over time, hence, we only show the global sensitivity analysis at time step 600 months. Similar to the before injection period, we do not observe significant correlations among parameters, hence, we only show the total sensitivity index (see Figure 4b). The global sensitivity analysis with the total thermal energy, and the total thermal and kinetic energy objective functions during injection period produce the same sensitivity results as the one before the injection period. They indicate the system undergoes the same physical processes before and during the injection period.

Using total kinetic energy objective function, we obtain the same significant parameters as the use of total entropy production objective function, however, with different total and first-order sensitivity values. Note that, the calculation of pressure requires fluid density, which is a function of temperature. Hence, $\lambda_N, \lambda_{CK}, \lambda_{KN}, \lambda_S, Q$, significant parameters identified using total thermal energy objective function, emerge as significant here. Since $\lambda_N, \lambda_{CK}, \lambda_{KN}, \lambda_S, Q$ do not directly affect the pressure, the total and first-order sensitivity values are less

than the one with total thermal energy objective function. In Darcy's law, permeability explicitly appears in pressure calculation, therefore, the significance of permeability k is the highest. The significance of k here is higher than the one from total entropy production objective function because the total entropy production objective function account for contributions of both the thermal and hydraulic component. While the global sensitivity analysis with total entropy production for all time steps during the injection period are the same as the one before injection period. It again indicates that the system undergoes the same physical processes until 600 months.

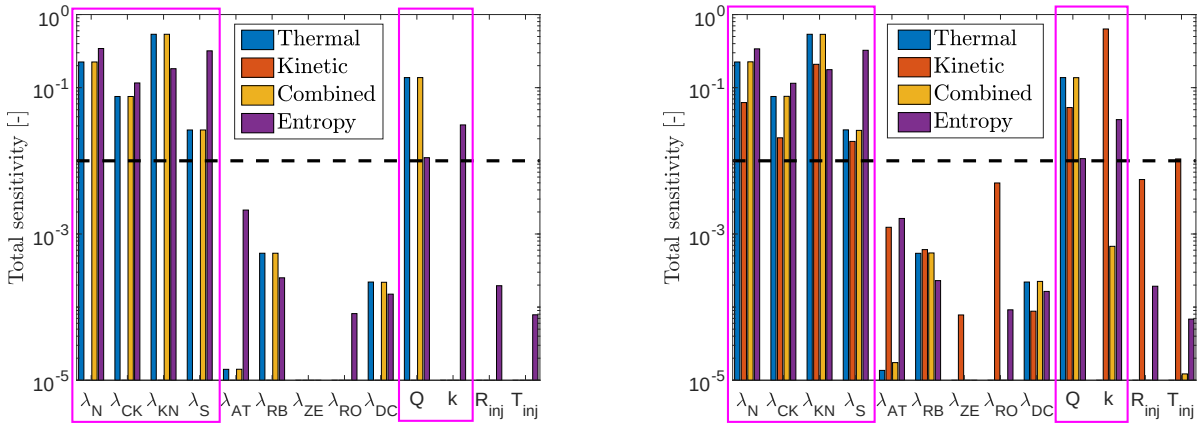

Figure 4: The total sensitivity index obtained through global sensitivity analysis with different objective functions: (a) before injection period, and (b) during injection period t = 600 months. The sensitivity results using the total thermal energy, the total kinetic energy, the total thermal and kinetic energy, and the total entropy production as objective functions are denoted by thermal, kinetic, combined, and entropy consecutively. The pink boxes highlight the significant parameters.

4. DISCUSSIONS

The entropy production provides a comprehensive insight in the transient thermo-hydraulic process since it describes the state of a system based on the thermodynamics law. It combines the information from the pressure and the temperature state in a thermodynamical way, not just simply adding the pressure and temperature state as it is done in the combined objective function. Hence, the use of the entropy production as an objective function in global sensitivity analysis provides more information. The sensitivity results obtained with the total entropy production objective function fall between those of the total thermal energy and kinetic energy objectives. With the total thermal energy objective function, we can only identify $\lambda_N, \lambda_{CK}, \lambda_{KN}, \lambda_S, Q$ as significant parameters, strongly tied with the heat conduction process. With the total kinetic energy objective function, we additionally identify k as significant parameter. However, with this function, we cannot obtain any result before the injection period since there is no flow. This objective function can only highlight the fluid flow contribution. On the other hand, the total entropy production objective function captures both heat conduction and fluid flow contributions simultaneously. Therefore, the use of the entropy production as the objective function in global sensitivity analyses is suitable for capturing the transient thermo-hydraulic process.

The primary challenge in employing the entropy production as an objective function for global sensitivity analyses lies in the calculation of the gradients. As depicted in Equation 2, the entropy production requires the calculation of the pressure and the temperature gradients. If we calculate the entropy production using the pressure and the temperature solutions directly, the global sensitivity analysis becomes computationally intensive. This is because, in each realization, we must employ a finite-difference scheme on the spatio-temporal pressure and temperature solutions, leading to a long computational time. Alternatively, we could create a surrogate model using pre-calculated entropy production values. In this approach, entropy production is computed during the generation of the training samples. It is worth noting that the entropy production solution can exhibit significant spatial and temporal variations spanning almost four orders of magnitude, necessitating a log transformation. However, achieving a substantial reduction with the Proper Orthogonal Decomposition (POD) becomes challenging with this log transformation, resulting in an increased offline time. In our case, utilizing an entropy production surrogate model proves to be a more efficient strategy for global sensitivity analyses, especially considering the need for a considerable number of realizations to avoid statistical errors.

The Delft Sandstone experiences thermo-hydraulic process, indicated by significant contribution of λ_{KN} and k from the thermodynamic perspective. It undergoes the same physical process (involving contributions from both irreversible thermal and fluid flow friction components) until 600 months, as indicated by the constant total sensitivity index values across all time steps. If injection-production operations were to be conducted in this layer, we can anticipate no significant changes in the reservoir due to these operations.

5. CONCLUSIONS

A global sensitivity analysis with an entropy production objective function is essential for enhancing our understanding of the thermo-hydraulic processes in geothermal reservoirs. This analysis identifies significant parameters based on the thermodynamic state of the

system, taking into account the contributions of the irreversible thermal and the fluid flow friction. It outperforms the use of the pressure and the temperature states as objective functions in global sensitivity analyses for comprehending transient thermo-hydraulic processes.

Given the computational cost for conducting global sensitivity analyses, the use of the non-intrusive reduced basis method is essential. The non-intrusive reduced-basis method gives a significant speed-up in calculating the entropy production of a new case and ensures accurate predictions with a small number of training samples.

ACKNOWLEDGEMENT

We would like to acknowledge funding from the European Union's Horizon 2020 research and innovation programme under the Marie Skłodowska-Curie grant agreement No 956965.

REFERENCES

Abadi, M. et al.: Tensorflow: Large-Scale Machine Learning on Heterogeneous Systems, https://www.tensorflow.org/ (2015).

Beer, A., Gravatt, M., Renaud, T., Nicholson, R., Maclaren, O., Dekkers, K., O'Sullivan, J., Power, A., Popineau, J., and O'Sullivan, M.: Geologically Consistent Prior Parameter Distributions for Uncertainty Quantification of Geothermal Reservoirs, Proceedings, Forty-eighth Workshop on Geothermal Reservoir Engineering Stanford University, Stanford, California (2023).

Bejan, A.: Convection Heat Transfer, 4th edition. New Jersey: John Wiley & Sons, Inc. (2013).

Börsing, N., Wellmann, F., Niederau, J., and Regenauer-Lieb, K.: Entropy production in a box: Analysis of instabilities in confined hydrothermal systems, Water Resources Research, 53, (2017), 7716-7739.

Cacace, M., and Jacquey, A. B.: Flexible parallel implicit modelling of coupled thermal–hydraulic–mechanical processes in fractured rocks, Solid Earth, 8, (2017), 921-941.

Chen, P., and Ghattas, O.: Projected Stein Variational Gradient Descent, Proceedings, Advances in Neural Information Processing Systems 33, (2020).

Clauser, C.: Numerical Simulation of Reactive Flow in Hot Aquifers, 1st edition. Heidelberg: Springer-Verlag Berlin Heidelberg (2003).

Degen, D., Voullieme, D. C., Buiter, S., Franssen, H. H., Vereecken, H., Gonzales-Nicolas, A., Wellmann, F.: Perspectives of physics-based machine learning for geoscientific applications governed by partial differential equations, Geoscientific Model Development, 16, (2023), 7375-7409.

Degen, D., Veroy, K., and Wellmann, F.: Uncertainty quantification for basin-scale geothermal conduction models, Scientific Reports, 12, (2022), 4246.

Degen, D., Spooner, C., and Cacace, M.: Effects of transient processes for thermal simulations of the Central European Basin, Geoscientific Model Development, 14, (2021a), 1699-1719.

Degen, D., Spooner, C., Scheck-Wenderoth, M., and Cacace, M.: How biased are our models? – a case study of the alpine region, Geoscientific Model Development, 14, (2021b), 7133–7153.

Degen, D., Veroy, K., Freymark, J., Scheck-Wenderoth, M., Poulet, T., and Wellmann, F.: Global sensitivity analysis to optimize basin-scale conductive model calibration–A case study from the Upper Rhine Graben, Geothermics, 95, (2021c), 102413.

Falkner, S., Klein, A., and Hutter, F.: BOHB: Robust and Efficient Hyperparameter Optimization at Scale, arXiv:1807.01774, (2018).

Herman, J., and Usher, W.: SALib: An open-source Python library for Sensitivity Analysis, Journal of Open Source Software, 2, (2017), 97.

Hesthaven, J. S., and Ubbiali, S.: Non-intrusive reduced order modeling of nonlinear problems using neural networks, Journal of Computational Physics, 363, (2018), 55-78.

Karakaşlı, G.: bohb-hpo, https://github.com/goktug97/bohb-hpo (2020).

Kern, R. and Weisbrod, A.: Thermodynamics for Geologists. San Francisco: Freeman, Cooper Co. (1967).

Lindsay, A. D. et al.: 2.0 – MOOSE: Enabling massively parallel Multiphysics simulation, Software X, 20, (2022), 101202.

Huang, P. and Wellmann, F.: An Explanation to the Nusselt–Rayleigh Discrepancy in Naturally Convected Porous Media, Transport in Porous Media, 137, (2021), 195-214.

Mottaghy, D., Pechnig, R., and Vogt, C.: The geothermal project Den Haag: 3D numerical models for temperature prediction and reservoir simulation, Geothermics, 40, (2011), 199-210.

Niederau, J., Wellmann, J. F., and Borsing, N.: Analyzing the influence of correlation length in permeability on convective systems in heterogeneous aquifers using entropy production, Geothermal Energy, 7, (2019), 1-27.

Regenauer-Lieb, K., Karrech, A., Chua, H. T., Horowitz, F. G., and Yuen, D.: Time-dependent, irreversible entropy production and geodynamics, Philosophical Transaction of the Royal Society A, 368, (2010), 285-300.

Saltelli, A., Aleksankina, K., Becker, W., Fennell, P., Ferretti, F., Holdst, N., Li, S., and Wu, Q.: Why so many published sensitivity analyses are false: A systematic review of sensitivity analysis practices, Environmental Modelling & Software, 114, (2019), 29 – 39.

Saltelli, A.: Making best use of model evaluations to compute sensitivity indices, Computer Physics Communications, 145, (2002), 280-297.

Schulte, D. O., Arnold, D., Geiger, S., Demyanov, V., and Sass, I.: Multi-objective optimization under uncertainty of geothermal reservoirs using experimental design-based proxy models, Geothermics, 86, (2020), 101792.

Sobol, I. M.: Global sensitivity indices for nonlinear mathematical models and their Monte Carlo estimates, Mathematics and Computers in Simulation, 55, (2001), 271-280.

Swischuk, R., Mainini, L., Peherstorfer, B., and Willcox, K.: Projection-based model reduction: Formulations for physics-based machine learning, Computers & Fluids, 179, (2019), 704-717.

Veldkamp, J. G., Loeve, D., Peters, E., Nair, R., Pizzocolo, F., and Wilschut, F.: Thermal fracturing due to low injection temperatures in geothermal doublets, TNO Report, 2015R11739, (2016), 1 – 42.

Vogt, C., Mottaghy, D., Wolf, A., Rath, V., Pechnig, R., and Clauser, C.: Reducing temperature uncertainties by stochastic geothermal reservoir modelling, Geophysical Journal International, 181, (2010), 321-333.

Wainwright, H. M., Finsterle, S., Jung, Y., Zhou, Q., and Birkholzer, J. T.: Making sense of global sensitivity analyses, Computers & Geosciences, 65, (2014), 84 – 94.

Wang, Q., Hesthaven, J., and Ray, D.: Non-intrusive reduced order modeling of unsteady flows using artificial neural networks with application to a combustion problem, Journal of Computational Physics, 384, (2019), 289-307.

Wellmann, J. F. and Regeneuer-Lieb, K.: EFFECT OF GEOLOGICAL DATA QUALITY ON UNCERTAINTIES IN GEOLOGICAL MODELS AND SUBSURFACE FLOW FIELDS, Proceedings, Thirty-Seventh Workshop on Geothermal Reservoir Engineering Stanford University, Stanford, California (2012).

Willcox, K., Ghattas, O., and Heimbach, P.: The imperative of physics-based modeling and inverse theory in computational science, Nature Computational Science, 1, (2021), 166-168.

Willems, C. J. L., Vondrak, A., Mijnlieff, H. F., Donselaar, M .E., and van Kempen, B. M. M.: Geology of the Upper Jurassic to Lower Cretaceous geothermal aquifers in the West Netherlands Basin – an overview, Netherlands Journal of Geosciences, 99, (2020), 1-13.